Extrasolar Kuiper Belts

Mark C. Wyatt

Abstract Extrasolar debris disks are the dust disks found around nearby main sequence stars arising from the break-up of asteroids and comets orbiting the stars. Far-IR surveys (e.g., with *Herschel*) showed that $\sim 20\%$ of stars host detectable dust levels. While dust temperatures suggest a location at 10s of au comparable with our Kuiper belt, orders of magnitude more dust is required implying a planetesimal population more comparable with the primordial Kuiper belt. High resolution imaging (e.g., with ALMA) has mapped the nearest and brightest disks, providing evidence for structures shaped by an underlying planetary system. Some of these are analogous to structures in our own Kuiper belt (e.g., the hot and cold classical, resonant, scattered disk and cometary populations), while others have no Solar System counterpart. CO gas is seen in some debris disks, and inferred to originate in the destruction of planetesimals with a similar volatile-rich composition to Solar System comets. This chapter reviews our understanding of extrasolar Kuiper belts and of how our own Kuiper belt compares with those of neighbouring stars.

1 Introduction

As the other chapters in this book testify, studies of the Kuiper belt continue to play a key role in shaping our understanding of the structure and history of the Solar System. This chapter aims to provide some context to this relatively detailed information on our own planetary system, by considering how this compares to the planetary systems of other stars, in particular with regard to the component of their debris disks which might be considered analogous to the Kuiper belt. Such comparisons help to ascertain whether our system is typical or atypical, either in terms of its current architecture, or in terms of its past history. They also allow a deeper

Mark C. Wyatt
Institute of Astronomy, University of Cambridge, Madingley Road, Cambridge CB3 0HA, United Kingdom, e-mail: wyatt@ast.cam.ac.uk

understanding of processes inferred to have occurred in our own history, since those processes may be ongoing for some stars, furthermore providing evidence for how these play out in different environments.

By now it is clear that our Solar System is just one of many planetary systems, with observations of nearby stars showing that approximately half of stars have a planetary system in which at least one of its planets may be detected in current surveys (Winn and Fabrycky 2015). However, this seemingly abundant information is restricted to the planets that reside close to their stars (within a few au), and information about the outer regions of planetary systems remains scarce. Indeed just a few percent of stars have planets $\gg 5$ au detectable by direct imaging (which means at least a few times more massive than Jupiter), although microlensing surveys hint that Neptune-analogues may be more common.

In contrast, our understanding of the dust content of outer planetary systems is relatively well advanced (e.g., Wyatt 2008; Hughes et al. 2018). It is over 30 years since the far-IR satellite *IRAS* first discovered circumstellar dust orbiting nearby main sequence stars (Aumann et al. 1984). Because this dust is short-lived it was recognised that it must be continually replenished from larger planetesimals situated in a source region that was inferred from the dust temperature to be at 10s of au (Backman and Paresce 1993), a conclusion that was reinforced by imaging of the dust structures (Smith and Terrile 1984). Stars with such dust have been called Vega-type (after the first discovery), and the circumstellar dust is referred to as a debris disk [1], and often interpreted to arise from an extrasolar analogue to the Solar System's Kuiper belt (e.g., Wyatt et al. 2003; Moro-Martín et al. 2008).

The extent to which that analogy is appropriate remains open for interpretation, but what is clear is that $\sim 20\%$ of stars have dust, and so presumably also planetesimals, at somewhere around 20-150 au from their stars (Wyatt 2008; Hughes et al. 2018). Given the aforementioned difficulty of detecting planets in these outer regions, it is usually uncertain whether this dust lies at the outer edge of a planetary system or whether there are other similarities with our own Kuiper belt, but there are clues in the dust structures. These often reinforce the Solar System analogy, with the caveat that there is some anthropocentric bias in this interpretation.

This chapter starts in §2 by summarising the various observational methods used to obtain information about these putative extrasolar Kuiper belts, then in §3 considers how our Solar System fits within this context. More detail is given in §4 about specific aspects about the physical and dynamical properties of the extrasolar systems and their comparison with the Solar System, before concluding in §5.

[1] Here *debris* refers to the debris left over after planet formation, which applies to any circumstellar material that is not a planet. This could include a dust or gas component left over from the protoplanetary disk, but also planetesimals and the dust and gas resulting from their destruction.

2 Extrasolar Kuiper Belt Observations

As noted in §1, most of the information about extrasolar Kuiper belts comes from observations of dust created in the destruction of their planetesimals. These observations can be roughly split into those used to discover the presence of dust using photometry (discussed in §2.1) and those that provide more detailed characterisation through high resolution imaging (discussed in §2.2). There is also an emerging area of observations of gas in the systems (see §2.3).

2.1 Discovery: Photometry and SED Fitting

Debris disk dust is most readily detected from its thermal emission which manifests itself as the star appearing brighter than expected from purely photospheric emission at wavelengths that depend on the dust temperature, although care must be taken to ensure that potential extragalactic contamination has been removed from the photometry (e.g., Kennedy and Wyatt 2012; Gáspár and Rieke 2014). The emission from dust created at 10s of au peaks at far-IR wavelengths and that is where the majority of debris disks have been discovered. The most recent surveys were those undertaken by *Herschel* (Eiroa et al. 2013; Matthews et al. 2014; Hughes et al. 2018), including an unbiased survey of the nearest several hundred stars in which dust emission was detected around 20% of stars (Thureau et al. 2014; Sibthorpe et al. 2018).

These photometric surveys are supplemented by photometry at mid-IR and submm wavelengths to build up the spectral energy distribution (SED) of the dust emission, which generally shows that the emission is dominated by a single temperature and so dust at a single distance (see e.g. Fig. 1). Given the luminosity of the star this can be translated into a black body distance (i.e., the distance at which the dust would be if it behaved like a black body), although it is recognised that the small dust that dominates is an inefficient emitter and so this is likely an underestimate of the true location of the dust by a factor that can be several depending on the star (Booth et al. 2013; Pawellek et al. 2014). In addition to its black body radius $r_{\rm bb}$, the disk's SED is also characterised by its fractional luminosity f (i.e., the luminosity of the dust divided by that of the star), with values of 10^{-6} to 10^{-3} typical for known disks.

For some systems the SED has been characterised in greater detail, in which case more realistic modelling is performed to constrain the dust size distribution and composition (e.g., Olofsson et al. 2012; Lebreton et al. 2012). However, the simple shape of the spectrum means that there is still value in considering the disks in terms of their two observable parameters ($r_{\rm bb}$ and f), particularly because there are a number of observational biases that can be readily understood within this context (Wyatt 2008). Nevertheless, some systems have an SED that is best characterised as having two temperatures (Chen et al. 2006; Kennedy and Wyatt 2014). In the context of an extrasolar Kuiper belt interpretation, this means that there is an additional

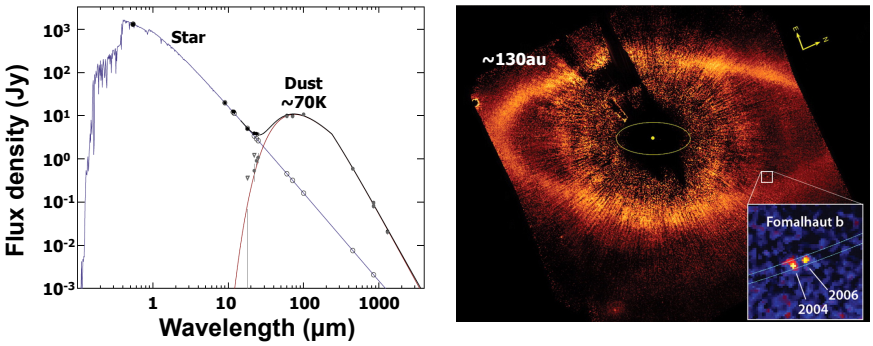

Fig. 1 Observations of the nearby (7.8 pc) 400 Myr A-type main sequence star Fomalhaut. *(Left)* Photometric observations show that the spectral energy distribution is comprised of two temperature components, one from the star and another from cold dust at ~ 70 K. *(Right)* Optical images in which the stellar emission has been subtracted using coronagraphic techniques to reveal scattered light from circumstellar dust that is distributed in a narrow ring at ~ 130 au from the star (Kalas et al. 2008). The centre of this ring is offset from the star implying an eccentricity of ~ 0.11, and a planet-like object (Fomalhaut-b) is seen close to the inner edge of the ring.

warm component of emission that might be analogous to the Solar System's zodiacal cloud. However, there remains debate about whether this component originates in an extrasolar asteroid belt analogue (Su et al. 2013), exocomets scattered in from the extrasolar Kuiper belt (Wyatt et al. 2017), or is a transient dust component perhaps caused by a recent collision (Jackson and Wyatt 2012).

2.2 Characterisation: Imaging

Debris disks around the nearest stars have a spatial extent of > 1 arcsec which means that these can be readily resolved. The low resolution of far-IR instrumentation precludes this except in a few cases (e.g., Acke et al. 2012), but this technique has been successful at optical and near-IR wavelengths with *HST* (see Fig. 1), and more recently SPHERE on VLT and GPI on Gemini, where starlight scattered by the smallest sub-μm dust can be imaged (e.g., Schneider et al. 2014). In the sub-mm with ALMA (Atacama Large Millimeter/submillimeter Array), thermal emission from mm to cm-sized grains can be imaged as well (see Fig. 5). Given the size of dust dominating the emission at the different wavelengths, it is generally assumed that sub-mm observations trace the distribution of the parent planetesimals, while the picture is more complicated at optical wavelengths because the orbits of small dust grains are significantly modified by radiation forces. Indeed, different radial and even nonaxisymmetric structures are seen in multiwavelength imaging of the same disk providing a valuable diagnostic tool for the underlying dynamics.

Such imaging provided the first evidence that the dust is configured in a disk (rather than a spherical distribution, Smith and Terrile 1984), and has allowed direct

measurement of the radial location of the dust, its radial and vertical extents and the presence of gaps (see §4.4), as well as providing evidence for asymmetries in the form of clumps, eccentricities and warps (see §4.5). All of these give vital clues to the underlying dynamics and the existence of planets.

2.3 Gas

Debris disks used to be considered as gas-free, in contrast to the protoplanetary disks found around young stars (< 10 Myr). Recent discoveries with ALMA show that this can no longer be considered the case, since there are now of order 10 main sequence stars known to exhibit CO gas emission. Many of the first gas detections are around the more massive A-type stars (Kóspál et al. 2013; Greaves et al. 2016; Moór et al. 2017), though there are a number of observational biases that facilitate the detection of gas around early-type stars, and gas is now seen around later spectral types as well (Marino et al. 2016; Matrà et al. 2019a). Most of these observations can be explained within the context of a model in which the gas in debris disks, like the dust, is the product of of the destruction of planetesimals that are then required to be volatile-rich (Kral et al. 2017). An open question is whether the youngest (< 50 Myr) stars retain gas from the protoplanetary disk phase (Kóspál et al. 2013; Kral et al. 2019). Observations of debris disk gas not only allow the mass and composition of gas to be measured (see §4.3), but also spatially resolved with additional kinematic information, resulting in a potentially powerful probe of the disk structure and dynamics (see §4.5, Dent et al. 2014).

3 An Extrasolar Perspective of the Kuiper Belt

It is important to note that the Solar System's debris disk is fainter than any known debris disk around another star. If one of the stars in the debris disk surveys hosted an exact replica of the Solar System, it would only have been possible to detect the photospheric emission from the star and not that of circumstellar dust (see Figs. 2 and 3). The challenge with detecting a true Kuiper belt analogue lies in the fact that its thermal emission is outshined by more than an order of magnitude at all wavelengths by the Sun.

In fact the level of thermal emission from dust in the Kuiper belt is not well known. Its emission has not been detected since it is masked by that of the zodiacal cloud which is much closer to the Earth, although the far-IR all-sky surveys like *IRAS*, *COBE* and *Planck* do provide upper limits on the level of emission that can be present (e.g., Backman et al. 1995). Direct detection of dust grains in the outer Solar System gives an indication of the number of dust grains present (Piquette et al. 2019), but this must be combined with dynamical models for dust production and evolution to understand the whole dust structure (Vitense et al. 2014). In doing so,

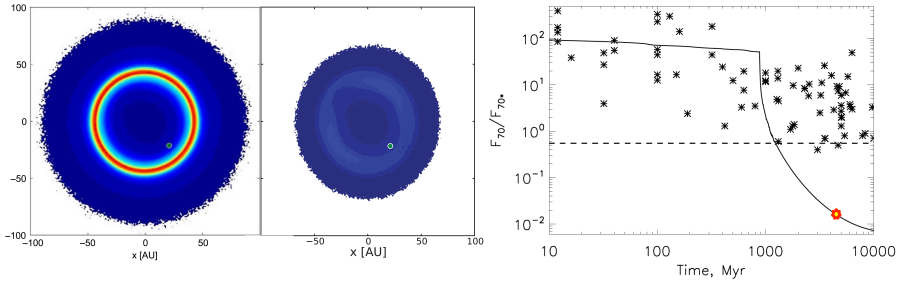

Fig. 2 The Solar System's Kuiper belt. *(Left)* Face-on images of the number density distribution of Kuiper belt objects that have been debiased from the observed distributions. To the left is shown the full Kuiper belt which appears as a narrow ring dominated by the classical Kuiper belt objects (Matthews and Kavelaars 2016), and to the right the contribution of resonant Kuiper belt objects that shows two clumps at $\pm 90^\circ$ from Neptune (shown with a circle) due to the Plutino population (Lawler 2014). *(Right)* The evolution of the 70 μm emission from dust in the Kuiper belt (shown as its level compared with that from the Sun) expected in the model of Gomes et al. (2005), and compared with the dust emission from nearby Sun-like stars (Booth et al. 2009). In this model the massive primordial Kuiper belt is comparable in brightness to those observed around nearby stars (shown with asterisks), but is depleted to a non-detectable level at $\sim$ 800 Myr by the Late Heavy Bombardment.

the best estimate is that Kuiper belt emission peaks at $\sim 70\,\mu$m at a flux 1% that of the Sun (Vitense et al. 2012). Even for bright stars their far-IR fluxes cannot be predicted with such accuracy, which combined with calibration uncertainties in photometric measurements, means that $\gg 10\%$ excesses are required for a confident detection.

If it were possible to resolve the emission from Kuiper belt dust, the structures that would be observed at long wavelengths would resemble the structures known to be present in the distribution of Kuiper belt objects (e.g., Lawler 2014); i.e., there would be a prominent ring at ~ 40 au from the classical Kuiper belt (see Fig. 2 left), with some non-axisymmetric structure caused by the resonant Kuiper Belt Objects (see Fig. 2 middle), and with emission extending out to larger radii from the scattered disk (which is present but hardly noticeable in Fig. 2 left). Given the low density of the dust distribution, the smallest dust (as traced by the shorter far-IR wavelengths) would migrate in by Poynting-Robertson drag and so fill in the 40 au hole. However, very little dust would make it past Jupiter or even Saturn, meaning that this tenuous dust distribution would have drops in density associated with these planets (Liou and Zook 1999; Moro-Martín and Malhotra 2002).

There are, however, indications that the Kuiper belt was more massive in the past by several orders of magnitude. At such an epoch there would have been correspondingly more dust, resulting in detectable levels of emission (see Fig. 2 right, Booth et al. 2009). Thus the known debris disks could be analogues to the primordial Kuiper belt, and thus representative of systems that either never will, or have yet to undergo, large-scale instabilities. Note though that the exact timing of the depletion in the Solar System remains uncertain (e.g., Gomes et al. 2005; Morbidelli et al. 2018).

4 Extrasolar Kuiper Belt Properties (and Comparison with Solar System)

4.1 Mass and Radius Distribution

Far-IR surveys from the past few decades have provided large quantities of information on the incidence of debris disks, as measured by the excess emission above photospheric levels at different wavelengths (typically at 24, 70, 100 and 160 μm). Surveys have been carried out for nearby stars with a variety of spectral types, distances and ages. While main sequence star ages are usually quite inaccurate, there is sufficient information, particularly when comparing associations of young stars for which ages can be better determined, to show that disks tend to get fainter with age (Rieke et al. 2005; Su et al. 2006). As such the surveys are usually interpreted within the context of population models that take collisional erosion into account (see §4.2).

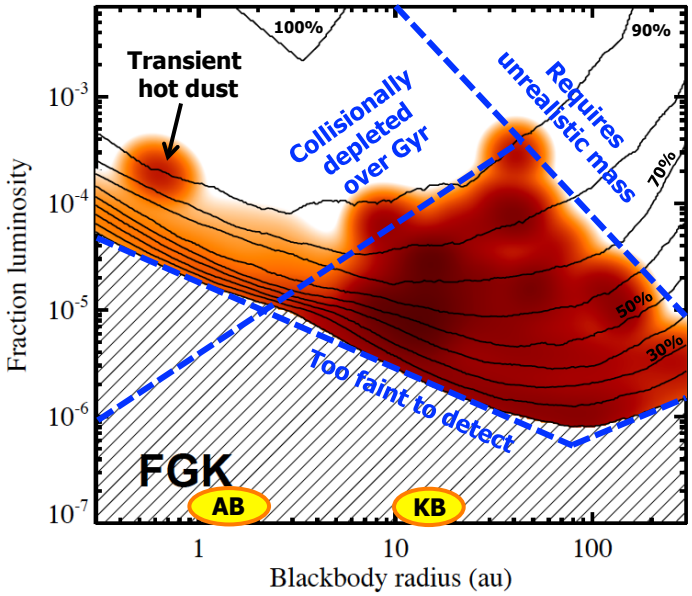

Fig. 3 Distribution of debris disk luminosities and radii (figure adapted from Sibthorpe et al. 2018). The colour scale shows the fraction of a sample of $\sim$ 300 Sun-like (FGK) stars from Phillips et al. (2010) that have dust emission as a function of their measured fractional luminosities and black body radii. The approximate locations of asteroid belt and Kuiper belt dust are shown in yellow, noting that the black body radius is a factor of a few smaller than the true radius because dust emits hotter than black body. The contours show the fraction of stars in the sample for which dust emission could have been detected, which is used to correct the observed incidence of debris to get the fraction plotted in the colour scale. The blue dashed lines and annotation explain why the known disks (which are present around $\sim$ 20% of stars) lie mostly in a well defined region of parameter space.

Fig. 3 summarises the state of our knowledge of the debris disk population seen around nearby Sun-like (i.e., F, G or K-type) stars. For each of the ~ 300 stars in the sample, the various observations (be they detections or non-detections of dust emission) have been combined to determine the best fit fractional luminosity and black body radius to their disk (see Fig. 1), or the upper limit on the dust luminosity for a given temperature to allow a non-detection. Particularly where disks are only detected at a single wavelength the fitted parameters can have significant uncertainty, and so the disks are placed on this plot accordingly [2], and the colour scale shows the fraction of stars in the sample predicted to have a disk in different regions of parameter space (for more details on the method, see Sibthorpe et al. 2018). Since observational biases mean that disks of a given level could only have been detected around a fraction of the stars in the sample as shown in the contours (Wyatt 2008), this is taken into account to get an estimate of the underlying distribution.

As noted in the figure, the distribution of known disks is bounded on the bottom edge by an observational limitation, while the top edges are set by physical considerations. For disks close to the star (< 40 au in black body radius) the maximum fractional luminosity is set by collisional erosion, since most nearby stars have the same roughly Gyr age and so their disks would be expected to have undergone similar levels of collisional processing and would have undergone more depletion the closer they are to the star (Wyatt et al. 2007b). Some disks may exhibit higher fractional luminosities if there happens to be a young star in the sample, or if there is a transient dust component (Wyatt et al. 2007a). For disks further from the star, the upper edge is set by a constraint on the mass required to produce the given fractional luminosity.

While Fig. 3 gives a quick visual impression of the distribution of debris disk properties, population models that also address the age dependence of the phenomenon can be used to get a more accurate parameterisation for the distributions of initial masses and radii of the disks. Such models show that it is possible to fit the observations by assuming that all stars started out with a planetesimal belt, with a radius and initial mass chosen from given distributions, that mass then evolving with time due to collisional erosion (Wyatt et al. 2007b; Löhne et al. 2008; Gáspár et al. 2013; Sibthorpe et al. 2018), although it is possible that a few of the brightest disks may require unrealistic initial masses ($\sim 1000 M_\oplus$, Krivov et al. 2018). There is evidence that the disks of A-type stars tend to be brighter than their Sun-like star counterparts (Greaves and Wyatt 2003), even accounting for the various biases (such as the on average younger ages of the more massive stars), which may be because of a difference in their planetesimal belt properties (e.g., in having more massive disks, or one made of smaller planetesimals, or lower levels of stirring). Given that many of the well known bright debris disks discussed in this review are found around A stars (like β Pic), it may be worth bearing this caveat in mind when making comparisons with the Solar System. There are few disks detected around the less massive M stars, but this is likely an observational bias and there is no evidence as yet to say

[2] More specifically, uncertainties in the photometric data mean that analysis of the spectral energy distribution can only determine a probability that the disk is present in a given part of fractional luminosity vs black body radius parameter space.

that their disks are any different to those of Sun-like stars (e.g., Morey and Lestrade 2014).

Despite the success of these models, it is worth noting that they cannot make any strong conclusions about the 80% of stars that do not have detectable disks, since these would be based on assumptions about the shape of the distributions. For example, a common assumption is that the mass distribution is log-normal, with the non-detections arising from close-in disks that undergo rapid depletion and so are not detectable in the nearby star population, but it could be that the mass distribution is bimodal, with 80% of stars having no disk. Also, more recently a correlation has been found between planetesimal belt radii determined from high resolution imaging of the sub-mm dust emission and the luminosity of the star (Matrà et al. 2018a). If this holds up as more disks are resolved, this would suggest a preferential location for the formation of planetesimal belts that could be linked to ice-lines in the protoplanetary disk for example, which would provide an additional constraint on the population models (as well as significant insight into the origin of the belts).

Fig. 3 also includes the location of the Solar System's Kuiper belt and Asteroid belt (see §3). This shows that roughly 20% of stars have disks that are comparable in radius to the Kuiper belt, in having dust at temperatures that give a black body radius of 10-100 au, but that have at least an order of magnitude more dust at fractional luminosities of 10^{-6} to 10^{-3}. For the reasons noted above it is not possible to quantify where our own Kuiper belt fits into the distribution.

4.2 Evolution: Collisional vs Dynamical Erosion

As noted in §4.1, the evidence that there is any evolution in debris disk properties comes not from seeing those changes in any one system, but rather from seeing the change in properties for samples of stars with different ages. Inevitably then there remains uncertainty in how individual disks evolve. However, since it is necessary for collisions to occur to replenish the dust that is observed, and that dust is lost from the system relatively quickly (compared with the age of the star), some level of collisional erosion is unavoidable. That evolution has been studied extensively both analytically and numerically, in ways that have also been applied to small body populations in the Solar System. In the Solar System evidence for past collisional evolution can be found in the detailed shape of the asteroid and Kuiper belt size distributions (e.g., Bottke et al. 2005; Fraser 2009; Singer et al. 2019), whereas in extrasolar systems the evolution of the size distribution in debris disks is manifested in the evolution of disk brightness which must be inferred from the population studies.

There are several unknowns in the problem, such as the initial size distribution of the planetesimals, their level of stirring (i.e., their collision velocity), and their size-dependent dispersal threshold. With these factors known, the collisional evolution would be well understood (e.g., Wyatt et al. 2011), and when coupled with models for dust optical properties that determine both its emission properties and loss due

to radiation forces, this can be readily translated into an evolution in the disk's observables. In principle this means that these fundamental physical parameters can be extracted from the observations, although in practise there are degeneracies between the parameters which make it hard to extract unambiguous information, other than that the vast majority of observations are consistent with purely steady state collisional erosion.

Indeed it is easier to identify the disk properties or processes that are incompatible with the observations, at least on a population level. For example, a slow decline in disk incidence with age that is consistent with collisional erosion means that large scale dynamical depletions at 100s of Myr must be relatively rare (Booth et al. 2009), otherwise there would be fewer bright disks at several Gyr ages. Thus either the Kuiper belt is anomalous in this respect (i.e., if its depletion is responsible for the Late Heavy Bombardment, Gomes et al. 2005), or the depletion actually occurred much earlier on (Morbidelli et al. 2018). It is also possible to conclude that the majority of debris disks are not broad planetesimal disks (even if each is only bright at one radius at any given time, e.g., Kenyon and Bromley 2010), since broad disks are hot early on and cold later on in a manner that is incompatible with the observed 24 and 70 μm brightness evolution (Kennedy and Wyatt 2010, see also §4.4).

However, for comparison with the Kuiper belt it is interesting to consider what has been concluded about the largest planetesimals in debris disks and the origin and level of stirring within them. While observations are only sensitive to dust up to $\sim$cm-size, the short collisional lifetime of such dust means that it must be continually replenished. Extrapolating the size distribution and equating the resulting collisional lifetime with age of the star shows that debris disks are replenished by planetesimals at least several km in size (Wyatt and Dent 2002), with population models pointing to sizes up to 100 km (Gáspár et al. 2013). It has been suggested that some disks may be comprised of much smaller planetesimals, say 10-100 m, that are colliding at very low velocity so that the collisions are barely disruptive (Heng and Tremaine 2010; Krivov et al. 2013), explaining the lack of small grains inferred to some systems (Eiroa et al. 2011), although chance alignment of background galaxies could be confusing the interpretation of these stars (Gáspár and Rieke 2014). Detailed observations of the halo of small grains seen to extend beyond a debris disk due to radiation pressure has the potential to constrain the level of stirring, with eccentricities inferred to be $< 1\%$ in one system (Thébault and Wu 2008). For some disks the vertical structure has been measured with inclinations inferred to be of order a few percent (Matrà et al. 2019b; Daley et al. 2019).

The origin of the stirring is not well constrained. It could arise from large bodies embedded in the disk that excite relative velocities to around their escape velocity (Kenyon and Bromley 2010). However, the growth of Pluto-sized objects at 100s of au in the disk takes too long to explain large disks seen around Gyr-old stars. One possibility is that these form directly from the protoplanetary disk (rather than from the collisional growth of smaller planetesimals), or it could be that a massive disk of ~ 200 km planetesimals can stir itself without the need for larger bodies (Krivov and Booth 2018). If the belts do mark the outer edge of the planetary system then

those planets could stir the disk through their gravitational perturbations. This could be through overlapping resonances from a planet at the inner edge (Quillen and Faber 2006), but could also arise from the secular perturbations of a more distant eccentric or inclined planet (Mustill and Wyatt 2009). It is also possible that the planetesimals were born on stirred orbits, e.g. if these formed in the early phases of the protoplanetary disk (Booth and Clarke 2016).

To illustrate the range of interpretations for debris disks that do not encompass a traditional Kuiper belt-like analogy, note that in one model the planetesimals form during protoplanetary disk dispersal from the dust that is swept up by a photoevaporating gas disk (Carrera et al. 2017). While such a model does not recover the observed distribution of debris disk radii, it is worth bearing in mind that our understanding of protoplanetary disk dispersal processes is incomplete, in particular regarding the fate of the $> 1 M_{\oplus}$ of mm-sized dust that resides in the outer regions of the system (Wyatt et al. 2015). As such it is not inconceivable that our understanding of the origin and evolution of debris disks could need revision.

4.3 Planetesimal Composition

A standard way of determining the composition of circumstellar material is to look for solid state features in the emission spectrum, such as the silicate features near $10\,\mu$m. This has been successful for the few systems for which warm dust is present (e.g., Lisse et al. 2009), however for the majority that are too cold to have significant mid-IR emission, this leaves far-IR features of which only a few were measured with *Herschel*. Nevertheless, when applied to the disk of β Pic, the $69\,\mu$m feature was used to show that 3.6% of the dust mass is in crystalline olivine grains, moreover constraining them to be relatively Mg-rich (de Vries et al. 2012).

As noted in §2.3, a new technique has been developed to probe the volatile content of the planetesimals by studying gas in the systems. Molecular gas has a short and well defined lifetime in optically thin environments since it is destroyed by interstellar radiation, e.g., CO has a lifetime of just ~ 120 years. Thus if a disk is observed to have a certain mass of CO, the rate at which CO is being replenished can be readily inferred. Since observations of the dust disk can also be used to determine the rate at which the refractory component is being replenished, these two rates can be used to find the volatile fraction of the planetesimals feeding the cascade. While there are some assumptions in that calculation, such as that both gas and dust are being replenished from steady state grinding, and the uncertainties in the CO mass measurement can be large if excitation conditions are not known (e.g., Matrà et al. 2015), this at least provides an order of magnitude estimate.

For now this has been achieved for a handful of disks with conclusions being that the fraction of the planetesimals that is made up of CO and CO_2 is similar to that of Solar System comets (see Fig. 4, Marino et al. 2016; Matrà et al. 2017b). Moreover the same model also explains those systems for which CO is not detected (Kral et al. 2017). Thus it is plausible that all debris disks are made of volatile-

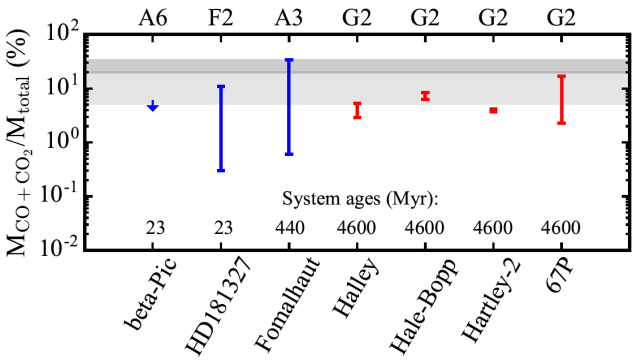

Fig. 4 Planetesimal volatile fraction inferred from observations of gas in debris disks compared with the same fractions for Solar System comets (Matrà et al. 2017b). Volatile fraction here is defined as the fraction of the total mass that is made up of CO and CO_2.

rich planetesimals, and so that all have associated secondary gas disks, but that only a fraction of these have CO at detectable levels. While no other gas molecules have been detected in debris disks, this is to be expected given the lower abundance relative to CO and moreover the even shorter lifetime of most molecules (Matrà et al. 2018b).

Atomic gas in the form of CI, CII and OI has also been detected (e.g., Riviere-Marichalar et al. 2014; Higuchi et al. 2017), where it is inferred that this gas is the photodissociation product of CO and CO_2. These are much longer lived and survive until the atomic gas disk has undergone viscous diffusion to be accreted onto the star (Kral et al. 2016). The observed ratio of carbon to CO thus constrains the viscous diffusion timescale, with implications for the underlying physics of that accretion (Kral and Latter 2016). For β Pic, this resulted in a prediction for the amount of OI that was too low compared with that observed, which was used to infer that the planetesimals were also water-rich, similar to Solar System comets, since that would explain the detection (Kral et al. 2016).

While there is an emerging paradigm that has been outlined above, it is worth noting that there remain uncertainties. For example, the model does not explain the distribution of CI observed in β Pic (Cataldi et al. 2018). It was also suggested that the < 50 Myr systems with protoplanetary disk levels of CO have a component of primordial gas that has yet to disperse (Kóspál et al. 2013; Moór et al. 2017). However, it was recently shown that such high levels of CO could be explained in a secondary production scenario, since if the gas production rate is particularly high, or the viscous diffusion timescale is too long, then sufficient carbon can accumulate to shield the CO from photodissociating, which then can also start to self-shield (Kral et al. 2019).

In consideration of the Solar System, the points to take away are that the volatile-rich composition of our Kuiper belt may be similar for other stars, and also that there may have been a tenuous atomic gas disk present early on.

4.4 Radial and Vertical Structure

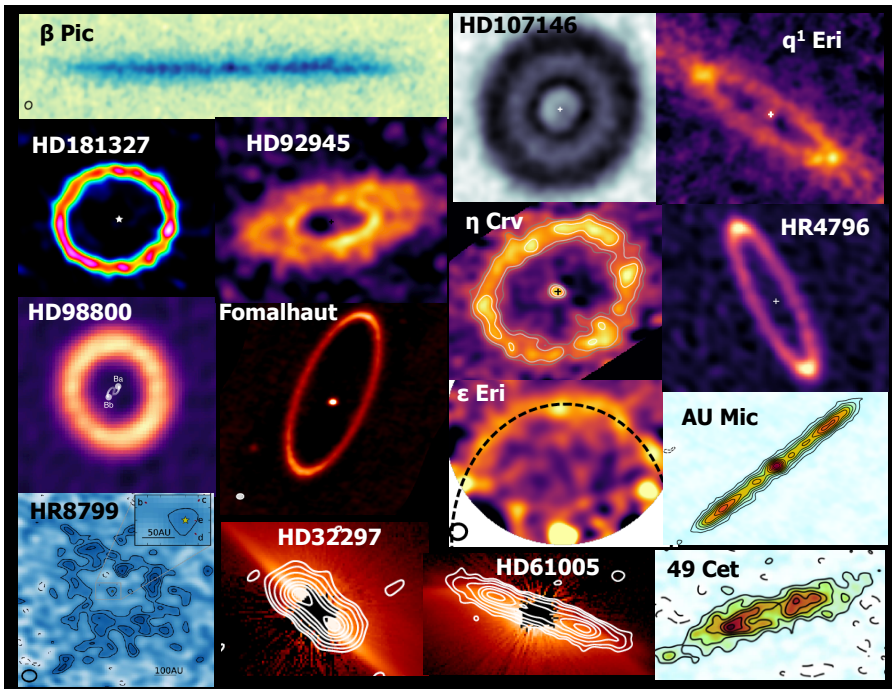

Fig. 5 Compilation of ALMA images of the distribution of mm-cm-sized dust in the debris disks of 15 nearby stars. Individual images are from: β Pic (Matrà et al. 2019b), HD107146 (Marino et al. 2018b), q^1 Eri (J. Lovell, private communication), HD181327 (Marino et al. 2016), HD92945 (Marino et al. 2019), η Crv (Marino et al. 2017b), HR4796 (Kennedy et al. 2018), HD98800 (Kennedy et al. 2019), Fomalhaut (MacGregor et al. 2017), ε Eri (Booth et al. 2017), AU Mic (Daley et al. 2019), HR8799 (Booth et al. 2016), HD32297 and HD61005 (Schneider et al. 2014; MacGregor et al. 2018), 49 Cet (Hughes et al. 2017).

As Fig. 1 shows, debris disks can be radially very narrow, with a fractional radial width (i.e., $\Delta r/r$) of $\sim 10\%$ in the example shown of the Fomalhaut disk. That width can be measured for disks that have been imaged, but more specifically requires that disks be resolved at mm wavelengths to determine the width of the planetesimal belt, since the smaller dust probed at shorter wavelengths will be spread out from the parent belt by radiation forces. There is then some bias in the sense that a broad disk will have lower surface brightness than a narrow one, and so will be harder to detect in high resolution imaging. Nevertheless, Fig. 5 shows that it is generally found that the disks are perhaps better described as rings or belts, with the fractional radial width ranging from 10-100%.

There are some notable exceptions to this description in that some disks are broad (e.g., MacGregor et al. 2016). For example, the 61 Vir disk extends from 30 au to

beyond 150 au (Wyatt et al. 2012; Marino et al. 2017a), a property which means that its surface brightness is so low that it is barely noticeable in ALMA imaging (but detected in the visibility data), with a radial profile that may be explained by a broad disk of ~ 10 km-sized planetesimals undergoing collisional erosion (Marino et al. 2017a). Other examples of broad disks include HD107146 and HD92945, which also show an annular gap in the radial profile (see Fig. 5, Marino et al. 2018b, 2019) that may be related to planets either embedded in the disk or nearby (Yelverton and Kennedy 2018).

The inner edges of the debris belts have received some attention, since it is noted that if the belt is truncated by dynamical interactions with a planet located at the inner edge, then the sharpness of the belt edge is indicative of the mass of the planet (e.g., Chiang et al. 2009). A more massive planet stirs up the disk to a greater extent resulting in a shallower slope. Analogy with the Solar System shows that the sharpness and location of the disk's outer edge can also be an important indicator of the system's past history (Gladman et al. 2001).

The outer edge of a debris disk is sometimes quoted as the location at which the disk becomes too faint to detect. However, it is expected that for planetesimals confined to a belt, there would be a halo of small μm-sized dust that extends beyond the belt due to radiation pressure (Strubbe and Chiang 2006). In this case the outer edge of the planetesimal belt would be evident as the location where there is a drop in the disk's surface brightness. However, it is now becoming clear that the extended dust components in some systems that were thought to be a halo of small dust also contain mm-sized dust (MacGregor et al. 2018). Since this dust is unlikely to be affected by radiation pressure, this calls into question whether the planetesimal disk is in fact broad with simply a step change in density at what had been assumed to be the outer edge of a radially confined planetesimal belt. The presence of a faint outer belt of debris in one system could support this view (Marino et al. 2016). Alternatively the extended halo of mm-sized grains could represent an analogue of the scattered disk, i.e., made of planetesimals (and the dust derived from their destruction) that are on eccentric orbits undergoing scattering with a planet located near the inner edge. Indeed the favoured interpretation of the radial structure of the HR8799 disk is that it has a low eccentricity disk (i.e., a classical Kuiper belt analogue) as well as a high eccentricity population of comets in a scattered disk analogue (see Fig. 6, Geiler et al. 2019), an interpretation strengthened by the fact that multiple planets interior to the belt are known in this system (Marois et al. 2010).

It was already noted in §4.2 that the vertical structure of some disks has now been resolved. Furthermore, for β Pic it was found that the vertical structure was not well described by a single Gaussian, rather it is fit well as the sum of two Gaussians that correspond to components with mean inclinations of 1° and 9° (Matrà et al. 2019b). While this is a few times flatter than the Solar System, there is a clear analogy with the cold and hot components of the classical Kuiper belt (see Fig. 6).

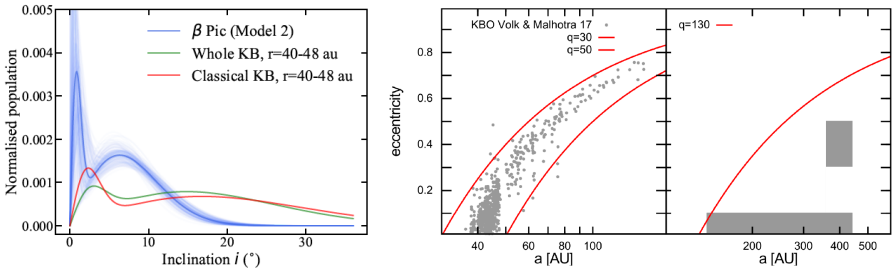

Fig. 6 Distributions of orbital elements inferred from ALMA images of debris disks that are analogous to dynamical populations in the Kuiper belt. *(Left)* Vertical structure in the β Pic disk (see Fig. 5) is best modelled as the the sum of two Gaussians that imply a distribution of inclinations reminiscent of the hot and cold classical Kuiper belt (Matrà et al. 2019b). *(Right)* Radial structure in the HR8799 disk (see Fig. 5) includes a halo of mm-sized grains that is best modelled with a high eccentricity population potentially analogous to the scattered disk (Geiler et al. 2019).

4.5 Dynamical Structures

Some of the radial structures discussed in §4.4 can be considered dynamical structures, in that the shape of inner and outer disk edges, and gaps within the disks, can all be related to the presence of planets. However, such an interpretation is potentially ambiguous, because this may alternatively be indicative of the initial distribution of planetesimals, in which radial structure may have been imprinted by processes ongoing during the protoplanetary disk phase (e.g., the formation of planetesimals at ice-lines); i.e., no planets may be required. Non-axisymmetric structure is a clearer indicator that additional perturbations are ongoing, since these would be needed to maintain such structures over long timescales.

Several of the disks that have been imaged are seen to be eccentric. This was manifested originally by a brightness asymmetry in mid-IR images of the HR4796 disk (Telesco et al. 2000), which was interpreted as arising from the pericentre side of the disk being closer to the star and so hotter and brighter (Wyatt et al. 1999). That interpretation is supported by ALMA imaging which showed that the opposite side of the disk is brighter (Kennedy et al. 2018) as expected due to the slower orbital velocity at apocentre (Pan et al. 2016). Subsequently scattered light imaging showed that the star is not exactly at the centre of the disk (Milli et al. 2017), although the direction of the offset is not exactly that expected suggesting that there may be some additional density variations around the ring (see also Löhne et al. 2017). Fomalhaut's disk (see Fig. 1) is perhaps a better example, being brighter and larger on the sky so that the offset and asymmetries are more clearly seen (Kalas et al. 2005; MacGregor et al. 2017), with additional azimuthal structure also evident (Kalas et al. 2013).

The origin of these eccentricities, which are of order 0.05-0.15, have not been identified, but would arise naturally from the secular perturbations of a planet on an eccentric orbit. While a planet candidate was detected orbiting near the inner edge of the Fomalhaut disk (see Fig. 1, Kalas et al. 2008) its eccentricity was subsequently

found to put it on a disk-crossing orbit (Kalas et al. 2013) that would significantly disrupt the disk suggesting that the planet is less massive than originally thought and/or has only been put on this orbit recently (Beust et al. 2014; Tamayo 2014; Lawler et al. 2015). The presence of an additional planet in the system that is responsible for the eccentricity is thus inferred.

A more secure identification of a disk asymmetry that is caused by planetary perturbations is the warp in the β Pic disk (Mouillet et al. 1997). The change in the plane of symmetry seen in scattered light images at 80 au in this edge-on disk (see Apai et al. 2015) was inferred to arise from the secular perturbations of a planet on an inclined orbit at ~ 10 au. Since that planet has subsequently been found with direct imaging (Lagrange et al. 2010), this supports the idea that disk structures can be used to identify unseen planets. That said, there remains some uncertainty in the interpretation of the vertical structure of the β Pic disk, not least because the additional clumpy structure mentioned below is situated at the same location as the warp.

Both the Vega and ε Eri debris disks were inferred to be clumpy based on sub-mm imaging (Holland et al. 1998; Greaves et al. 1998). Subsequent imaging gave conflicting views on the presence of the clumps (Greaves et al. 2005; Marsh et al. 2006; Hughes et al. 2012; Holland et al. 2017), but it seems likely that at least some of the clumpiness was attributable to background galaxies. The most secure evidence for clumpiness in a disk comes from β Pic for which mid-IR images show a prominent clump at ~ 50 au in projected separation from the star (Telesco et al. 2005). The same clump was later imaged in CO (see Fig. 7, Dent et al. 2014), for which the additional kinematic information showed that the clump is both radially and azimuthally broad and situated at ~ 85 au distance from the star (Matrà et al. 2017a). Two models were proposed to explain the clump, either a recent collision between two Mars-sized protoplanets (Jackson et al. 2014), or the trapping of planetesimals into the 2:1 and 3:2 resonances of a $\sim 30 M_\oplus$ planet that migrated out from 31-57 au over 23 Myr (Wyatt 2003; Matrà et al. 2019b). The radial breadth of the clump disfavours a collisional origin leaving the favoured interpretation as a structure analogous to the resonant Kuiper belt objects (the Plutinos and Twotinos). Comparison of Figs. 2 and 7 show there are some notable differences, however, such as that the tight clump observed in the β Pic disk would require the planetesimals to have a smaller libration width than resonant objects in the Kuiper belt. This could be explained within the context of this model by the stochasticity of the migration and/or the initial orbital eccentricities (e.g., Reche et al. 2008; Nesvorný and Vokrouhlický 2016).

4.6 Connection from Outer to Inner System

The fraction of stars with excess 10 μm emission indicative of warm dust in the region where there may be habitable planets was long recognised to be low (Aumann and Probst 1991), and was quantified more recently from the WISE photometric

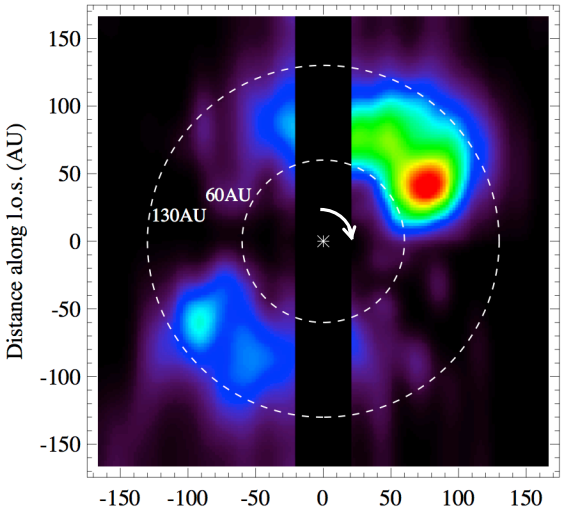

Fig. 7 Dynamical structure in the debris disk of β Pic that is analogous to that of resonant Kuiper belt objects. While the disk is edge-on, velocity information from CO observations allows its face-on distribution to be inferred showing that this includes two clumps of unequal brightness on opposite sides of the star (Dent et al. 2014). The best explanation is that outward migration of a planet close to the inner edge of the disk trapped volatile-rich planetesimals into its 2:1 and 3:2 resonances causing over-densities in these regions where collisions are most frequent (Wyatt 2003). The CO lifetime is short compared with the orbital timescale meaning that it does not travel far from where it is created before being photodissociated.

survey to find that excesses above 10% of the stellar emission only occur to 1:10^4 nearby stars (Kennedy and Wyatt 2013), although this rate is higher if considering a sample of young < 100 Myr stars. This result is explained by collisional evolution (see also Fig. 3 and §4.1, Wyatt et al. 2007a), which suggests that the rare bright excesses are transient populations of warm dust, perhaps originating in recent collisions. However, ongoing interferometric surveys have shown that excesses at 0.1-1% levels are more common, and present to $\sim$ 20% of stars (Ertel et al. 2018), and moreover are more prevalent (though not exclusively) around stars known to host cold outer disks (Mennesson et al. 2014).

This does not prove that the warm dust must originate somehow in the outer belt, since it could be that the conditions of a protoplanetary disk that leads to the formation of an outer cold belt also favour the formation of a massive asteroid belt (e.g., Geiler and Krivov 2017). However, there are two mechanisms by which outer belts can replenish a warm dust population. The first is by Poynting-Robertson drag (Burns et al. 1979). While the dust population dragged in from the known outer belts is expected to be significantly depleted by mutual collisions (which is not the case in the more tenuous belt in the Solar System, Wyatt 2005), the levels of dust expected to make it in to $\sim$ 1 au are comparable to those inferred from observations in some cases (Mennesson et al. 2014; Kennedy and Piette 2015), although the dust population may be further depleted if the dust has to cross the path of any planets

(Bonsor et al. 2018). The second is by comet scattering. That is, an intervening planetary system could scatter planetesimals into the inner regions where they could sublimate or disintegrate to replenish the warm dust, much as comets in the Solar System replenish the zodiacal cloud (Nesvorný et al. 2010).

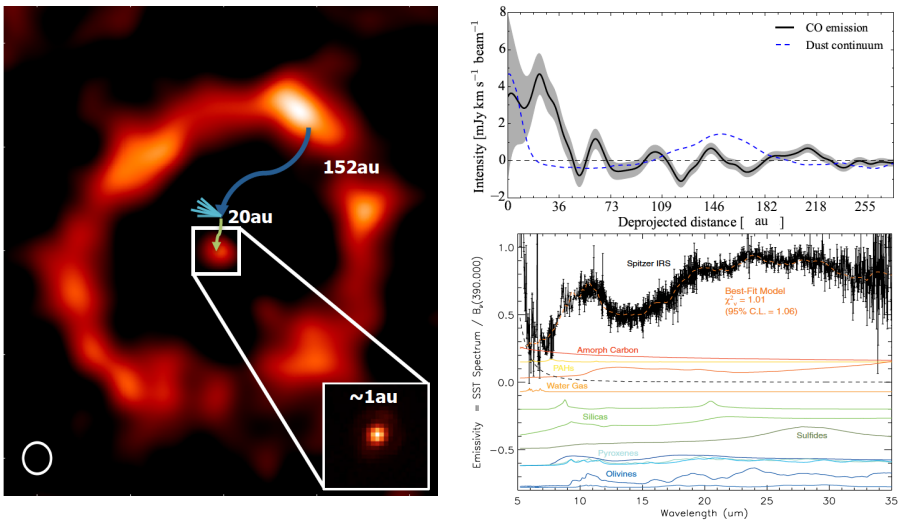

Fig. 8 Evidence for inward scattering of exocomets in the debris disk of the ~ 1 Gyr F star η Crv. *(Left)* ALMA image of its outer debris belt (and the stellar photospheric emission at the centre), with inset (bottom right) of the mid-IR emission showing warm dust close to the star, and annotation to illustrate the origin of that warm dust in exocomet scattering (Marino et al. 2017b). *(Top right)* The profile of CO emission showing this peaks at ~ 20 au close to where the exocomets may be expected to cross the H_2O or CO_2 ice lines (Marino et al. 2017b). *(Bottom right)* The spectrum of mid-IR emission can be fitted by a model for the dust composition that suggests it is water- and carbon-rich (Lisse et al. 2012).

For η Crv shown in Fig. 8, its $\sim 10\%$ excess from dust at ~ 1 au (Smith et al. 2009; Defrère et al. 2015) cannot be explained by steady state collisions in an asteroid belt given its ~ 1 Gyr age (Wyatt et al. 2007a). In this case an origin in the outer belt seen at 150 au (Wyatt et al. 2005) is most likely, and is supported by the composition of the warm dust inferred from its infrared spectrum (Lisse et al. 2012). The warm dust is too bright to be explained by P-R drag, but inward scattering of comets is the favoured scenario, particularly following the tentative detection of CO gas at ~ 20 au from the star (Marino et al. 2017b). The detection of gas at a location where there is no dust is surprising, but is readily explained if this is the location where comets start sublimating on their way in before depositing their dust at ~ 1 au.

The requirement to sustain a high rate of comet scattering sets constraints on the intervening planetary system, e.g. since the comets should not be ejected before reaching the inner regions (Wyatt et al. 2017), but it is found that a plausible planetary system architecture is one with a chain of $3-30M_\oplus$ planets (Marino et al. 2017b). More generally, some level of comet scattering is expected in all systems

with an outer belt, with the rate determined by the processes that perturb planetesimals out of their orbits in the belt, and the architecture of their planetary system (Marino et al. 2018a). Since these planetesimals may impact any planets and so deliver water or strip their atmospheres, this has significant interest for those seeking to understand the prevalence of conditions that favour the development of life.

5 Conclusions

The Sun is not unique in having either a planetary system or in having belts of planetesimals. Other stars also have what can be considered as extrasolar analogues to the Kuiper belt. However, the extent of that analogy depends on how strict the similarities must be. Certainly other stars have belts of planetesimals at distances from their stars similar to our own Kuiper belt, but these belts contain orders of magnitude more mass, perhaps comparable to that in our primordial Kuiper belt. Since we cannot yet detect a true Kuiper belt analogue around another star we cannot yet tell how ours compares within the population, except to say that it is not in the top 20%.

There are, however, many other similarities to the Kuiper belt in the debris disks observed around other stars. For example, several have volatile-rich compositions inferred to be similar to Solar System comets (from gas observations). In terms of structures, there is evidence for analogues to the hot and cold classical belt (from vertically resolved edge-on disks), to the resonant Kuiper belt object population (from clumpy disks), and to the scattered disk (from haloes of mm-sized grains). Many disks are seen to be radially narrow with sharp inner and outer edges (from resolved imaging). It is also inferred that in some systems exocomets are scattered into the inner regions (from observations of close-in dust and gas).

It is nevertheless worth bearing in mind that these similarities are based in some cases on a relatively small number of what must inevitably be considered the extremes of the debris disk population (in that they are bright enough to have been studied in sufficient detail to identify any similarity). Also, the similarities that are highlighted in the literature (and in this review) reflect to some extent our inherently anthropocentric view (e.g., some of the aforementioned features may have other interpretations). Moreover, there are also examples of disks that do not fit into a Kuiper belt-like mold (e.g., the broad disks, or the eccentric rings).

These differences in the extrasolar debris disk population are to be expected, because just as we have learned by comparing the Solar System to the exoplanet population, planet formation has a diverse range of outcomes of which the Solar System is just one example. By studying and comparing our Kuiper belt to extrasolar debris disks, we have a different perspective on those outcomes, one which is biased towards processes that occur in the outer regions of the systems that are hard to access through exoplanet observations. What the similarities do show is that, perhaps, we share some dynamical processes in common with other stars, and by considering the

Solar System as one outcome we may achieve a deeper understanding of the planet formation process and the uniqueness of our own situation.

References

Acke B, Min M, Dominik C et al. (2012) Herschel images of Fomalhaut. An extrasolar Kuiper belt at the height of its dynamical activity. A&A540:A125

Apai D, Schneider G, Grady CA et al. (2015) The Inner Disk Structure, Disk-Planet Interactions, and Temporal Evolution in the β Pictoris System: A Two-epoch HST/STIS Coronagraphic Study. ApJ800:136

Aumann HH Probst RG (1991) Search for Vega-like nearby stars with 12 micron excess. ApJ368:264–271

Aumann HH, Gillett FC, Beichman CA et al. (1984) Discovery of a shell around Alpha Lyrae. ApJ278:L23–L27

Backman DE Paresce F (1993) Main-sequence stars with circumstellar solid material - The VEGA phenomenon. In: Levy EH Lunine JI (eds) Protostars and Planets III, pp 1253–1304

Backman DE, Dasgupta A Stencel RE (1995) Model of a Kuiper Belt Small Grain Population and Resulting Far-Infrared Emission. ApJ450:L35

Beust H, Augereau JC, Bonsor A et al. (2014) An independent determination of Fomalhaut b's orbit and the dynamical effects on the outer dust belt. A&A561:A43

Bonsor A, Wyatt MC, Kral Q et al. (2018) Using warm dust to constrain unseen planets. MNRAS480:5560–5579

Booth M, Wyatt MC, Morbidelli A, Moro-Martín A Levison HF (2009) The history of the Solar system's debris disc: observable properties of the Kuiper belt. MNRAS399:385–398

Booth M, Kennedy G, Sibthorpe B et al. (2013) Resolved debris discs around A stars in the Herschel DEBRIS survey. MNRAS428:1263–1280

Booth M, Jordán A, Casassus S et al. (2016) Resolving the planetesimal belt of HR 8799 with ALMA. MNRAS460:L10–L14

Booth M, Dent WRF, Jordán A et al. (2017) The Northern arc of ϵ Eridani's Debris Ring as seen by ALMA. MNRAS469:3200–3212

Booth RA Clarke CJ (2016) Collision velocity of dust grains in self-gravitating protoplanetary discs. MNRAS458:2676–2693

Bottke WF, Durda DD, Nesvorný D et al. (2005) The fossilized size distribution of the main asteroid belt. Icarus175:111–140

Burns JA, Lamy PL Soter S (1979) Radiation forces on small particles in the solar system. Icarus40:1–48

Carrera D, Gorti U, Johansen A Davies MB (2017) Planetesimal Formation by the Streaming Instability in a Photoevaporating Disk. ApJ839:16

Cataldi G, Brandeker A, Wu Y et al. (2018) ALMA Resolves C I Emission from the β Pictoris Debris Disk. ApJ861:72

Chen CH, Sargent BA, Bohac C et al. (2006) Spitzer IRS Spectroscopy of IRAS-discovered Debris Disks. ApJS166:351–377

Chiang E, Kite E, Kalas P, Graham JR Clampin M (2009) Fomalhaut's Debris Disk and Planet: Constraining the Mass of Fomalhaut b from disk Morphology. ApJ693:734–749

Daley C, Hughes AM, Carter ES et al. (2019) The Mass of Stirring Bodies in the AU Mic Debris Disk Inferred from Resolved Vertical Structure. ApJ875:87

de Vries BL, Acke B, Blommaert JADL et al. (2012) Comet-like mineralogy of olivine crystals in an extrasolar proto-Kuiper belt. Nature490:74–76

Defrère D, Hinz PM, Skemer AJ et al. (2015) First-light LBT Nulling Interferometric Observations: Warm Exozodiacal Dust Resolved within a Few AU of η Crv. ApJ799:42

Dent WRF, Wyatt MC, Roberge A et al. (2014) Molecular Gas Clumps from the Destruction of Icy Bodies in the β Pictoris Debris Disk. Science 343:1490–1492
Eiroa C, Marshall JP, Mora A et al. (2011) Herschel discovery of a new class of cold, faint debris discs. A&A536:L4
Eiroa C, Marshall JP, Mora A et al. (2013) DUst around NEarby Stars. The survey observational results. A&A555:A11
Ertel S, Defrère D, Hinz P et al. (2018) The HOSTS Survey - Exozodiacal Dust Measurements for 30 Stars. AJ155:194
Fraser WC (2009) The Collisional Divot in the Kuiper Belt Size Distribution. ApJ706:119–129
Gáspár A Rieke GH (2014) The Herschel Cold Debris Disks: Confusion with the Extragalactic Background at 160 μm. ApJ784:33
Gáspár A, Rieke GH Balog Z (2013) The Collisional Evolution of Debris Disks. ApJ768:25
Geiler F Krivov AV (2017) Does warm debris dust stem from asteroid belts? MNRAS468:959–970
Geiler F, Krivov AV, Booth M Löhne T (2019) The scattered disc of HR 8799. MNRAS483:332–341
Gladman B, Kavelaars JJ, Petit JM et al. (2001) The Structure of the Kuiper Belt: Size Distribution and Radial Extent. AJ122:1051–1066
Gomes R, Levison HF, Tsiganis K Morbidelli A (2005) Origin of the cataclysmic Late Heavy Bombardment period of the terrestrial planets. Nature435:466–469
Greaves JS Wyatt MC (2003) Some anomalies in the occurrence of debris discs around main-sequence A and G stars. MNRAS345:1212–1222
Greaves JS, Holland WS, Moriarty-Schieven G et al. (1998) A Dust Ring around ϵ Eridani: Analog to the Young Solar System. ApJ506:L133–L137
Greaves JS, Holland WS, Wyatt MC et al. (2005) Structure in the ϵ Eridani Debris Disk. ApJ619:L187–L190
Greaves JS, Holland WS, Matthews BC et al. (2016) Gas and dust around A-type stars at tens of Myr: signatures of cometary breakup. MNRAS461:3910–3917
Heng K Tremaine S (2010) Long-lived planetesimal discs. MNRAS401:867–889
Higuchi AE, Sato A, Tsukagoshi T et al. (2017) Detection of Submillimeter-wave [C I] Emission in Gaseous Debris Disks of 49 Ceti and β Pictoris. ApJ839:L14
Holland WS, Greaves JS, Zuckerman B et al. (1998) Submillimetre images of dusty debris around nearby stars. Nature392:788–791
Holland WS, Matthews BC, Kennedy GM et al. (2017) SONS: The JCMT legacy survey of debris discs in the submillimetre. MNRAS470:3606–3663
Hughes AM, Wilner DJ, Mason B et al. (2012) Confirming the Primarily Smooth Structure of the Vega Debris Disk at Millimeter Wavelengths. ApJ750:82
Hughes AM, Lieman-Sifry J, Flaherty KM et al. (2017) Radial Surface Density Profiles of Gas and Dust in the Debris Disk around 49 Ceti. ApJ839:86
Hughes AM, Duchêne G Matthews BC (2018) Debris Disks: Structure, Composition, and Variability. ARA&A56:541–591
Jackson AP Wyatt MC (2012) Debris from terrestrial planet formation: the Moon-forming collision. MNRAS425:657–679
Jackson AP, Wyatt MC, Bonsor A Veras D (2014) Debris froms giant impacts between planetary embryos at large orbital radii. MNRAS440:3757–3777
Kalas P, Graham JR Clampin M (2005) A planetary system as the origin of structure in Fomalhaut's dust belt. Nature435:1067–1070
Kalas P, Graham JR, Chiang E et al. (2008) Optical Images of an Exosolar Planet 25 Light-Years from Earth. Science 322:1345
Kalas P, Graham JR, Fitzgerald MP Clampin M (2013) STIS Coronagraphic Imaging of Fomalhaut: Main Belt Structure and the Orbit of Fomalhaut b. ApJ775:56
Kennedy GM Piette A (2015) Warm exo-Zodi from cool exo-Kuiper belts: the significance of P-R drag and the inference of intervening planets. MNRAS449:2304–2311
Kennedy GM Wyatt MC (2010) Are debris discs self-stirred? MNRAS405:1253–1270

Kennedy GM Wyatt MC (2012) Confusion limited surveys: using WISE to quantify the rarity of warm dust around Kepler stars. MNRAS426:91–107
Kennedy GM Wyatt MC (2013) The bright end of the exo-Zodi luminosity function: disc evolution and implications for exo-Earth detectability. MNRAS433:2334–2356
Kennedy GM Wyatt MC (2014) Do two-temperature debris discs have multiple belts? MNRAS444:3164–3182
Kennedy GM, Marino S, Matrà L et al. (2018) ALMA observations of the narrow HR 4796A debris ring. MNRAS475:4924–4938
Kennedy GM, Matrà L, Facchini S et al. (2019) A circumbinary protoplanetary disk in a polar configuration. Nature Astronomy 3:230–235
Kenyon SJ Bromley BC (2010) Variations on Debris Disks. II. Icy Planet Formation as a Function of the Bulk Properties and Initial Sizes of Planetesimals. ApJS188:242–279
Kóspál Á, Moór A, Juhász A et al. (2013) ALMA Observations of the Molecular Gas in the Debris Disk of the 30 Myr Old Star HD 21997. ApJ776:77
Kral Q Latter H (2016) The magnetorotational instability in debris-disc gas. MNRAS461:1614–1620
Kral Q, Wyatt M, Carswell RF et al. (2016) A self-consistent model for the evolution of the gas produced in the debris disc of β Pictoris. MNRAS461:845–858
Kral Q, Matrà L, Wyatt MC Kennedy GM (2017) Predictions for the secondary CO, C and O gas content of debris discs from the destruction of volatile-rich planetesimals. MNRAS469:521–550
Kral Q, Marino S, Wyatt MC, Kama M Matra L (2019) Imaging [CI] around HD 131835: reinterpreting young debris discs with protoplanetary disc levels of CO gas as shielded secondary discs. MNRAS489:3670–3691
Krivov AV Booth M (2018) Self-stirring of debris discs by planetesimals formed by pebble concentration. MNRAS479:3300–3307
Krivov AV, Eiroa C, Löhne T et al. (2013) Herschel's "Cold Debris Disks": Background Galaxies or Quiescent Rims of Planetary Systems? ApJ772:32
Krivov AV, Ide A, Löhne T, Johansen A Blum J (2018) Debris disc constraints on planetesimal formation. MNRAS474:2564–2575
Lagrange AM, Bonnefoy M, Chauvin G et al. (2010) A Giant Planet Imaged in the Disk of the Young Star β Pictoris. Science 329:57
Lawler SM (2014) The Debiased Kuiper Belt: Our Solar System as a Debris Disk. In: Booth M, Matthews BC Graham JR (eds) Exploring the Formation and Evolution of Planetary Systems, IAU Symposium, vol 299, pp 232–236, DOI 10.1017/S1743921313008466
Lawler SM, Greenstreet S Gladman B (2015) Fomalhaut b as a Dust Cloud: Frequent Collisions within the Fomalhaut Disk. ApJ802:L20
Lebreton J, Augereau JC, Thi WF et al. (2012) An icy Kuiper belt around the young solar-type star HD 181327. A&A539:A17
Liou JC Zook HA (1999) Signatures of the Giant Planets Imprinted on the Edgeworth-Kuiper Belt Dust Disk. AJ118:580–590
Lisse CM, Chen CH, Wyatt MC et al. (2009) Abundant Circumstellar Silica Dust and SiO Gas Created by a Giant Hypervelocity Collision in the ˜12 Myr HD172555 System. ApJ701:2019–2032
Lisse CM, Wyatt MC, Chen CH et al. (2012) Spitzer Evidence for a Late-heavy Bombardment and the Formation of Ureilites in η Corvi at ˜1 Gyr. ApJ747:93
Löhne T, Krivov AV Rodmann J (2008) Long-Term Collisional Evolution of Debris Disks. ApJ673:1123–1137
Löhne T, Krivov AV, Kirchschlager F, Sende JA Wolf S (2017) Collisions and drag in debris discs with eccentric parent belts. A&A605:A7
MacGregor MA, Lawler SM, Wilner DJ et al. (2016) ALMA Observations of the Debris Disk of Solar Analog τ Ceti. ApJ828:113
MacGregor MA, Matrà L, Kalas P et al. (2017) A Complete ALMA Map of the Fomalhaut Debris Disk. ApJ842:8

MacGregor MA, Weinberger AJ, Hughes AM et al. (2018) ALMA Detection of Extended Millimeter Halos in the HD 32297 and HD 61005 Debris Disks. ApJ869:75
Marino S, Matrà L, Stark C et al. (2016) Exocometary gas in the HD 181327 debris ring. MNRAS460:2933–2944
Marino S, Wyatt MC, Kennedy GM et al. (2017a) ALMA observations of the multiplanet system 61 Vir: what lies outside super-Earth systems? MNRAS469:3518–3531
Marino S, Wyatt MC, Panić O et al. (2017b) ALMA observations of the η Corvi debris disc: inward scattering of CO-rich exocomets by a chain of 3-30 $M_\oplus$ planets? MNRAS465:2595–2615
Marino S, Bonsor A, Wyatt MC Kral Q (2018a) Scattering of exocomets by a planet chain: exozodi levels and the delivery of cometary material to inner planets. MNRAS479:1651–1671
Marino S, Carpenter J, Wyatt MC et al. (2018b) A gap in the planetesimal disc around HD 107146 and asymmetric warm dust emission revealed by ALMA. MNRAS479:5423–5439
Marino S, Yelverton B, Booth M et al. (2019) A gap in HD 92945's broad planetesimal disc revealed by ALMA. MNRAS484:1257–1269
Marois C, Zuckerman B, Konopacky QM, Macintosh B Barman T (2010) Images of a fourth planet orbiting HR 8799. Nature468:1080–1083
Marsh KA, Dowell CD, Velusamy T, Grogan K Beichman CA (2006) Images of the Vega Dust Ring at 350 and 450 μm: New Clues to the Trappingof Multiple-Sized Dust Particles in Planetary Resonances. ApJ646:L77–L80
Matrà L, Panić O, Wyatt MC Dent WRF (2015) CO mass upper limits in the Fomalhaut ring - the importance of NLTE excitation in debris discs and future prospects with ALMA. MNRAS447:3936–3947
Matrà L, Dent WRF, Wyatt MC et al. (2017a) Exocometary gas structure, origin and physical properties around β Pictoris through ALMA CO multitransition observations. MNRAS464:1415–1433
Matrà L, MacGregor MA, Kalas P et al. (2017b) Detection of Exocometary CO within the 440 Myr Old Fomalhaut Belt: A Similar CO+CO_2 Ice Abundance in Exocomets and Solar System Comets. ApJ842:9
Matrà L, Marino S, Kennedy GM et al. (2018a) An Empirical Planetesimal Belt Radius-Stellar Luminosity Relation. ApJ859:72
Matrà L, Wilner DJ, Öberg KI et al. (2018b) Molecular Reconnaissance of the β Pictoris Gas Disk with the SMA: A Low HCN/(CO+CO_2) Outgassing Ratio and Predictions for Future Surveys. ApJ853:147
Matrà L, Öberg KI, Wilner DJ, Olofsson J Bayo A (2019a) On the Ubiquity and Stellar Luminosity Dependence of Exocometary CO Gas: Detection around M Dwarf TWA 7. AJ157:117
Matrà L, Wyatt MC, Wilner DJ et al. (2019b) Kuiper Belt-like Hot and Cold Populations of Planetesimal Inclinations in the β Pictoris Belt Revealed by ALMA. AJ157:135
Matthews BC Kavelaars J (2016) Insights into Planet Formation from Debris Disks: I. The Solar System as an Archetype for Planetesimal Evolution. Space Sci Rev205:213–230
Matthews BC, Krivov AV, Wyatt MC, Bryden G Eiroa C (2014) Observations, Modeling, and Theory of Debris Disks. Protostars and Planets VI pp 521–544
Mennesson B, Millan-Gabet R, Serabyn E et al. (2014) Constraining the Exozodiacal Luminosity Function of Main-sequence Stars: Complete Results from the Keck Nuller Mid-infrared Surveys. ApJ797:119
Milli J, Vigan A, Mouillet D et al. (2017) Near-infrared scattered light properties of the HR 4796 A dust ring. A measured scattering phase function from 13.6° to 166.6°. A&A599:A108
Moór A, Curé M, Kóspál Á et al. (2017) Molecular Gas in Debris Disks around Young A-type Stars. ApJ849:123
Morbidelli A, Nesvorny D, Laurenz V et al. (2018) The timeline of the lunar bombardment: Revisited. Icarus305:262–276
Morey É Lestrade JF (2014) On the steady state collisional evolution of debris disks around M dwarfs. A&A565:A58
Moro-Martín A Malhotra R (2002) A Study of the Dynamics of Dust from the Kuiper Belt: Spatial Distribution and Spectral Energy Distribution. AJ124:2305–2321

Moro-Martín A, Wyatt MC, Malhotra R Trilling DE (2008) Extrasolar Kuiper Belt Dust Disks, pp 465–480
Mouillet D, Larwood JD, Papaloizou JCB Lagrange AM (1997) A planet on an inclined orbit as an explanation of the warp in the Beta Pictoris disc. MNRAS292:896
Mustill AJ Wyatt MC (2009) Debris disc stirring by secular perturbations from giant planets. MNRAS399:1403–1414
Nesvorný D Vokrouhlický D (2016) Neptune's Orbital Migration Was Grainy, Not Smooth. ApJ825:94
Nesvorný D, Jenniskens P, Levison HF et al. (2010) Cometary Origin of the Zodiacal Cloud and Carbonaceous Micrometeorites. Implications for Hot Debris Disks. ApJ713:816–836
Olofsson J, Juhász A, Henning T et al. (2012) Transient dust in warm debris disks. Detection of Fe-rich olivine grains. A&A542:A90
Pan M, Nesvold ER Kuchner MJ (2016) Apocenter Glow in Eccentric Debris Disks: Implications for Fomalhaut and ϵ Eridani. ApJ832:81
Pawellek N, Krivov AV, Marshall JP et al. (2014) Disk Radii and Grain Sizes in Herschel-resolved Debris Disks. ApJ792:65
Phillips NM, Greaves JS, Dent WRF et al. (2010) Target selection for the SUNS and DEBRIS surveys for debris discs in the solar neighbourhood. MNRAS403:1089–1101
Piquette M, Poppe AR, Bernardoni E et al. (2019) Student Dust Counter: Status report at 38 AU. Icarus321:116–125
Quillen AC Faber P (2006) Chaotic zone boundary for low free eccentricity particles near an eccentric planet. MNRAS373:1245–1250
Reche R, Beust H, Augereau JC Absil O (2008) On the observability of resonant structures in planetesimal disks due to planetary migration. A&A480:551–561
Rieke GH, Su KYL, Stansberry JA et al. (2005) Decay of Planetary Debris Disks. ApJ620:1010–1026
Riviere-Marichalar P, Barrado D, Montesinos B et al. (2014) Gas and dust in the beta Pictoris moving group as seen by the Herschel Space Observatory. A&A565:A68
Schneider G, Grady CA, Hines DC et al. (2014) Probing for Exoplanets Hiding in Dusty Debris Disks: Disk Imaging, Characterization, and Exploration with HST/STIS Multi-roll Coronagraphy. AJ148:59
Sibthorpe B, Kennedy GM, Wyatt MC et al. (2018) Analysis of the Herschel DEBRIS Sun-like star sample. MNRAS475:3046–3064
Singer KN, McKinnon WB, Gladman B et al. (2019) Impact craters on Pluto and Charon indicate a deficit of small Kuiper belt objects. Science 363:955–959
Smith BA Terrile RJ (1984) A circumstellar disk around Beta Pictoris. Science 226:1421–1424
Smith R, Wyatt MC Haniff CA (2009) Resolving the hot dust around HD69830 and η Corvi with MIDI and VISIR. A&A503:265–279
Strubbe LE Chiang EI (2006) Dust Dynamics, Surface Brightness Profiles, and Thermal Spectra of Debris Disks: The Case of AU Microscopii. ApJ648:652–665
Su KYL, Rieke GH, Stansberry JA et al. (2006) Debris Disk Evolution around A Stars. ApJ653:675–689
Su KYL, Rieke GH, Malhotra R et al. (2013) Asteroid Belts in Debris Disk Twins: Vega and Fomalhaut. ApJ763:118
Tamayo D (2014) Consequences of an eccentric orbit for Fomalhaut b. MNRAS438:3577–3586
Telesco CM, Fisher RS, Piña RK et al. (2000) Deep 10 and 18 Micron Imaging of the HR 4796A Circumstellar Disk: Transient Dust Particles and Tentative Evidence for a Brightness Asymmetry. ApJ530:329–341
Telesco CM, Fisher RS, Wyatt MC et al. (2005) Mid-infrared images of β Pictoris and the possible role of planetesimal collisions in the central disk. Nature433:133–136
Thébault P Wu Y (2008) Outer edges of debris discs. How sharp is sharp? A&A481:713–724
Thureau ND, Greaves JS, Matthews BC et al. (2014) An unbiased study of debris discs around A-type stars with Herschel. MNRAS445:2558–2573

Vitense C, Krivov AV, Kobayashi H Löhne T (2012) An improved model of the Edgeworth-Kuiper debris disk. A&A540:A30

Vitense C, Krivov AV Löhne T (2014) Will New Horizons See Dust Clumps in the Edgeworth-Kuiper Belt? AJ147:154

Winn JN Fabrycky DC (2015) The Occurrence and Architecture of Exoplanetary Systems. ARA&A53:409–447

Wyatt MC (2003) Resonant Trapping of Planetesimals by Planet Migration: Debris Disk Clumps and Vega's Similarity to the Solar System. ApJ598:1321–1340

Wyatt MC (2005) The insignificance of P-R drag in detectable extrasolar planetesimal belts. A&A433:1007–1012

Wyatt MC (2008) Evolution of Debris Disks. ARA&A 46:339–383

Wyatt MC Dent WRF (2002) Collisional processes in extrasolar planetesimal discs - dust clumps in Fomalhaut's debris disc. MNRAS334:589–607

Wyatt MC, Dermott SF, Telesco CM et al. (1999) How Observations of Circumstellar Disk Asymmetries Can Reveal Hidden Planets: Pericenter Glow and Its Application to the HR 4796 Disk. ApJ527:918–944

Wyatt MC, Holland WS, Greaves JS Dent WRF (2003) Extrasolar Analogues to the Kuiper Belt. Earth Moon and Planets 92:423–434

Wyatt MC, Greaves JS, Dent WRF Coulson IM (2005) Submillimeter Images of a Dusty Kuiper Belt around η Corvi. ApJ620:492–500

Wyatt MC, Smith R, Greaves JS et al. (2007a) Transience of Hot Dust around Sun-like Stars. ApJ658:569–583

Wyatt MC, Smith R, Su KYL et al. (2007b) Steady State Evolution of Debris Disks around A Stars. ApJ663:365–382

Wyatt MC, Clarke CJ Booth M (2011) Debris disk size distributions: steady state collisional evolution with Poynting-Robertson drag and other loss processes. Celestial Mechanics and Dynamical Astronomy 111:1–28

Wyatt MC, Kennedy G, Sibthorpe B et al. (2012) Herschel imaging of 61 Vir: implications for the prevalence of debris in low-mass planetary systems. MNRAS424:1206–1223

Wyatt MC, Panić O, Kennedy GM Matrà L (2015) Five steps in the evolution from protoplanetary to debris disk. Ap&SS357:103

Wyatt MC, Bonsor A, Jackson AP, Marino S Shannon A (2017) How to design a planetary system for different scattering outcomes: giant impact sweet spot, maximizing exocomets, scattered discs. MNRAS464:3385–3407

Yelverton B Kennedy GM (2018) Empty gaps? Depleting annular regions in debris discs by secular resonance with a two-planet system. MNRAS479:2673–2691